geographies

Article

Geomorphological and Neotectonic Structures Studied in the Southern Part of the Moesian Platform in Romania

Irina Stanciu [1,*] and Dumitru Ioane [2]

1 National Institute for Research and Development for Marine Geology and Geoecology—GeoEcoMar, 024053 Bucharest, Romania
2 Faculty of Geology and Geophysics, University of Bucharest, 020956 Bucharest, Romania; dumitru.ioane@g.unibuc.ro
* Correspondence: irina.stanciu@geoecomar.ro

Abstract: The Moesian Platform represents a major tectonic unit of the foreland of the Carpathians and Balkans, spanning across the southern part of Romania and the northern part of Bulgaria. Although the Moesian Platform is considered to be a stable tectonic unit, it has played a significant role in the geological history of the region, influencing the development of the surrounding Carpathian and Balkan mountain ranges, making it an area of interest for studying tectonic history, geological structures, and landscape evolution. In the southern part of the Moesian Platform in Romania, delineated to the north and to the east by the steep slopes of the Argeş River valley and to the south by the steep slopes of the Danube River valley, an elevated and W–E promontory-looking geomorphological feature identified by the local inhabitants as "hill" is distinct from the neighbouring flat relief of the Romanian plain. This study is the result of a comprehensive investigation into the geomorphological features and neotectonic structures within this region. An intriguing outcrop displaying a filled fault, cutting and displacing the Quaternary sedimentary formations of the recently named Argeş Promontory, shed light on recent tectonic activities that have influenced the landscape. By integrating field observations, geological, and tectonic data, as well as satellite geodetic data, our results contribute to a better understanding of the study area's regional geodynamics, emphasizing the significant role of tectonic activity in shaping the present-day landscape.

Keywords: Moesian Platform; Argeş Promontory; Crivăț Fault; active faulting; regional tectonics; regional geodynamics; geotectonic history

Citation: Stanciu, I.; Ioane, D. Geomorphological and Neotectonic Structures Studied in the Southern Part of the Moesian Platform in Romania. *Geographies* **2023**, *3*, 743–762. https://doi.org/10.3390/geographies3040040

Academic Editor: Gianluca Groppelli

Received: 8 September 2023
Revised: 24 October 2023
Accepted: 12 November 2023
Published: 20 November 2023

1. Introduction

The Moesian Platform (Figure 1) represents a major tectonic unit of the foreland of the Carpathians and Balkans, spanning across the southern part of Romania and the northern part of Bulgaria, in south-eastern Europe. It forms a W–E elongated, fault-delineated structural unit, extending into the Western Black Sea Basin up to the continental slope, where it gradually transitions into oceanic-type crust [1,2].

In Romania, the platform is considered to be separated from the Carpathian orogenic belt by the Pericarpathian Fault, while geophysical and borehole data suggest the northward prolongation of the platform deep underneath the Southern Carpathians and the East Carpathians Bend Zone [1–7]. The Moesian Platform extends up to the Trotuş Fault in the north and the Peceneaga-Camena Fault to the northeast [1,2]. Its western limit is delineated by the Timok Fault.

The main geomorphological feature of the Moesian Platform north of the Danube River is the Romanian plain.

In Bulgaria, the Balkans overthrust the southern margin of the platform along the Prebalkan Fault [8]. The main geomorphological feature of the Moesian Platform south of the Danube River is the Danube platform (comprising vast Quaternary structural lowlands and Pliocene platforms), also known as the Danubian hilly plain [9].

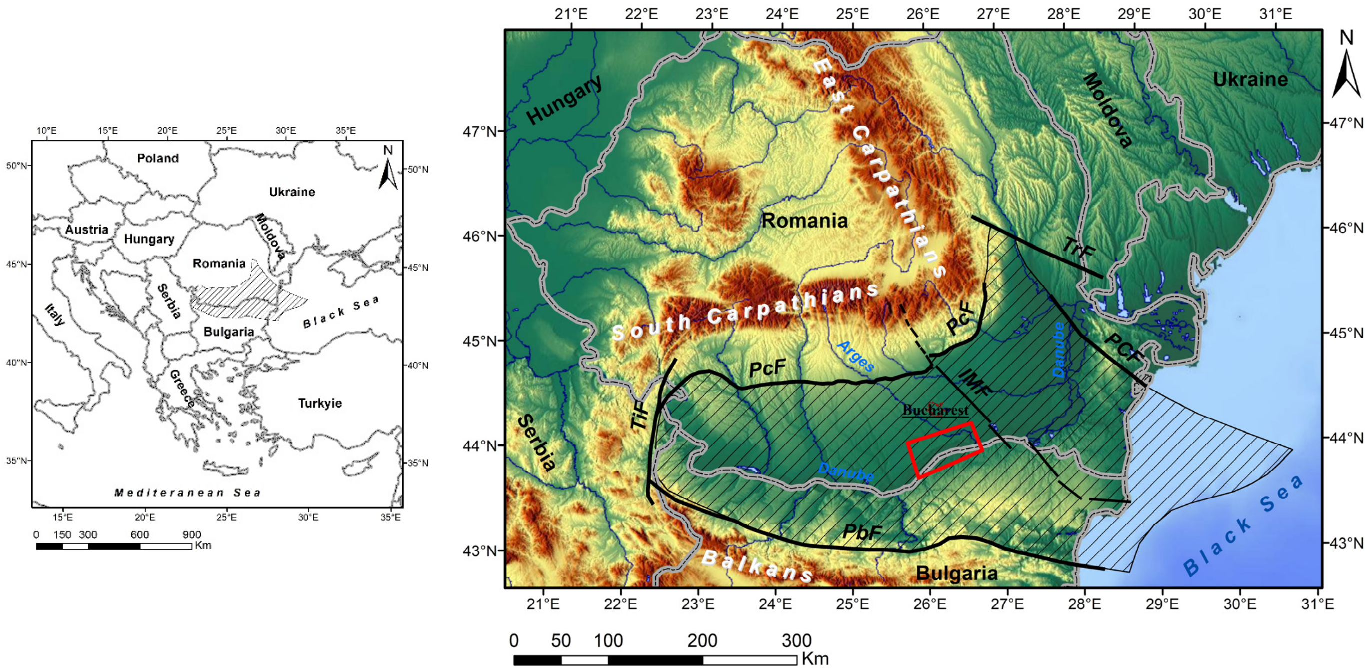

(**a**) (**b**)

Figure 1. The Moesian Platform: (**a**) location within south-eastern Europe; (**b**) tectonic sketch (modified and simplified after [1,2,10,11]). Hatched area = the Moesian Platform. Black lines = faults (PcF = Pericarpathian Fault; PbF = Prebalkan Fault; TrF = Trotuș Fault; TiF = Timok Fault; PCF = Peceneaga-Camena Fault; IMF = Intramoesian Fault). Red polygon = the Argeș Promontory area. Relief map modified after [12].

When addressing the Moesian Platform's geotectonic history, contrasting concepts have been carried out [13–31] due to scarce geological data on the basement, while the geophysical data did not clarify the structural relationships between the Moesian terranes.

Although it is considered to represent a stable tectonic unit, it has played a significant role in the geological history of the region: it is generally accepted that Moesia collided with the Carpathian-Balkan emerging orogens during the Cretaceous through the Miocene [32–35], with an essential role in the achievement of the Carpathian double-bend [1] (i.e., the first bend at the southern end of the East Carpathians and the second bend at the western end of the South Carpathians, as illustrated in Figure 1). The tectonic effort implied by the achievement of the Carpathian double-bend generated important extensional forces within the Moesian Platform during the Pliocene-Quaternary [36].

The Moesian Platform was intensively investigated starting in the mid-1950s due to its hydrocarbon resources. The most consistent information regarding the upper crustal structure in Moesia has been provided by refraction and reflection seismic surveys for oil and gas and from boreholes [4], continued by deep refraction seismic profiling studies reaching upper mantle depths [37–41].

The structural and morphological model of the crystalline basement built by Polonic [42] on seismic reflection and deep seismic sounding, integrated with borehole data, shows within the Romanian Moesian Platform uplifted structures (e.g., Central Dobrogea—outcropping, Balş-Optaşi region—ca. 4 km depth) and depressionary areas (such as the Alexandria Depression—more than 10 km depth, Focşani Depression—more than 16 km depth, Getic Depression—more than 14 km depth). Four main sedimentary cycles have been separated based on borehole geological and geophysical data analysis and correlations by D. Paraschiv [4,43]: Palaeozoic (Cambrian–Ordovician–Carboniferous), Upper Palaeozoic (Permian)–Lower Mesozoic (Triassic), Mesozoic (Jurassic–Cretaceous), and Cenozoic (Badenian–Pleistocene).

Starting in the 1990s, benefiting from advances in technology (i.e., the recording change from analogue to digital), crustal structure seismic investigations on the Carpathians and their foreland were carried out (e.g., the VRANCEA99 seismic refraction profile [40], deployed on ca. 320 km seismic refraction line, NNE–SSW-trending from Bacău to Bucharest; the VRANCEA 2001 seismic refraction profile [41], deployed from the Transylvanian Basin, over the Carpathian Orogen/Vrancea region, to the Moesian Platform/Focşani Depression and the North Dobrogea Orogen on a ca. 450 km long WNW–ESE-trending seismic refraction line), looking for regional structural and tectonic features in relation to the Vrancea region of the East Carpathians Bend Zone, Romania's strong intermediate-depth earthquakes prone area.

Several fault systems (see Figure 2) have been interpreted by various authors within the Moesian Platform based on geological and geophysical data [1–4,10,11,37,44–61]:

- a NW–SE (mainly) strike-slip fault system, relatively transverse to the East Carpathians Bend Zone, ranging from Palaeozoic to Cretaceous;
- an east–west normal fault system, parallel to the Carpathian and Balkan orogens;
- a NE–SW fault system, parallel to the East Carpathians Bend zone—younger (considered by Săndulescu [1] to have been generated and, in part, reactivated during Neogene), with normal and strike-slip faults;
- a N–S fault system.

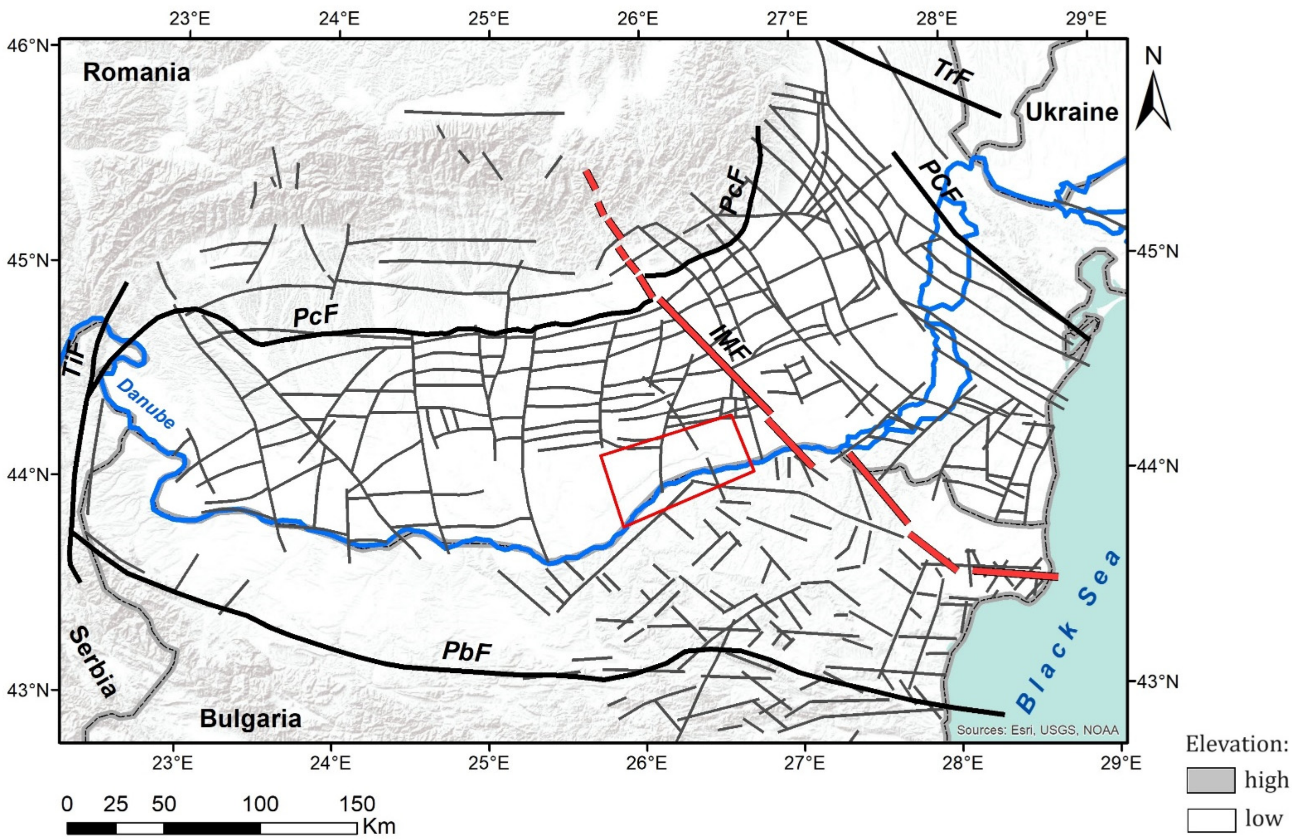

Figure 2. Tectonic sketch of the Moesian Platform (compiled from [1–4,10,11,37,44–61]). Thick black lines = Moesian Platform delineating faults (PcF = Pericarpathian Fault; PbF = Prebalkan Fault; TrF = Trotuș Fault; TiF = Timok Fault; PCF = Peceneaga-Camena Fault). Thick red line = Intramoesian Fault (IMF). Dark grey lines = faults. Red polygon = the Argeș Promontory area.

The platform plunges step-like below the Carpathian thrust wedge as well as below the Balkan thrust wedge, within the frame of the east–west parallel faults system.

Within the NW–SE fault system, the Intramoesian Fault (see Figure 1, IMF) represents a regional trans-crustal fault, which acts as a deep regional tectonic contact [11,62] between the two compartments of the Moesian Platform: Western Moesia (west of the Intramoesian Fault) and Eastern Moesia (east of the Intramoesian Fault).

Originating in the research for the “Intramoesian Fault: Geophysical detection and regional active (net)tectonics and geodynamics” PhD thesis [11], the Moesian Platform is an area of interest when addressing the geotectonic history of this region, its tectonic features, geological structures, and landscape evolution.

During field research carried out in 2019 in the southern part of the Moesian Platform in Romania, an elevated and W–E promontory-looking geomorphological feature came to our attention (for location, see Figure 1, red polygon). Delineated to the north and to the east by the steep slopes of the Argeş River valley and to the south by the steep slopes of the Danube River valley, this intriguing geomorphological feature, identified by the local inhabitants as “hill”, is distinct from the neighbouring flat relief of the Romanian plain.

By integrated analysis of field observations, geological and tectonic data, as well as satellite geodetic data, our research contributes to a better understanding of the study area’s regional geodynamics, emphasizing the significant role of tectonic activity in shaping the present-day landscape.

2. Data and Methods

Repeated field observations on the geological and geomorphological regional framework of the Moesian Platform in Romania and Bulgaria have been carried out during 2016–2023 in order to assess the regional active (neo)tectonics of the Moesian Platform, giving the opportunity to observe and analyse its geomorphological and neotectonic structures. The recently named Argeş Promontory [11], delineated to the north and to the east by the steep slopes of the Argeş River valley and to the south by the steep slopes of the Danube River valley, has been subject to yearly field visits starting in 2019, when the Crivăț Fault outcrop [11,63] was first observed. Field observations and measurements on the Crivăț Fault outcrop (i.e., GPS coordinates of the fault outcrop, strike and dip measurements, width of the fault zone, throw, roughness of the fault surface analysis, identifying slickensides, documenting the outcrop with photographs) helped in deciphering its characteristics and geometry.

Various types of geological and geotectonic data, geophysical data, repeated geodetic levelling, GNSS/GPS (Global Navigation Satellite System/Global Positioning System) data—from published thematic maps, scientific reports, studies, or scientific papers (all quoted accordingly and listed as references), have been included in our research and used in a referenced ESRI ArcGIS geo-database. This enabled an integrated approach to the interpretation of the available data.

Analysis of regional seismicity data available from published local, regional, and global earthquake catalogues offered the possibility to analyse the Moesian Platform’s seismicity, building the grounds for a better understanding of the seismic risk in this region.

Seismicity data analysis has been carried out based on the ROMPLUS Earthquake Catalogue [64], BIGSEES Selection of Earthquakes Catalogue [65], EMSC Earthquake Catalogue [66], ISC-GEM Global Instrumental Earthquake Catalogue [67], European-Mediterranean Earthquake Catalogue (EMEC) [68], Earthquake Catalogue for Central and Southeastern Europe 342 BC–1990 AD [69], SHARE European Earthquake Catalogue (SHEEC) 1000–1899 [70], SHEEC earthquake catalogue 1900–2006 [71], USGS Earthquake Catalogue [72], UNDP/UNESCO Survey of the Seismicity of the Balkan Region—Catalogue of Earthquakes [73]. Seismicity data have been compiled into a GIS database and carefully analysed. Earthquake recordings have been verified in order not to duplicate the seismic events.

Considering the large variety of earthquake catalogues, with different spatial coverage and timespan of the records, with possible different accuracies of the hypocentres’ determinations, the compatibility of seismological data became an important stage before data interpretation:

- For Romania and the Romanian Black Sea shore, the National Institute for Earth's Physics ROMPLUS Earthquake Catalogue [64] was used. We used the earthquake recordings from the time interval 984–2022.
- For Bulgaria and the Bulgarian Black Sea shore, an updated earthquake catalogue from Bulgaria was not available. The BIGSEES Selection of Earthquakes Catalogue [65] was considered the best option for the integrated study of the Romanian and Bulgarian parts of the Moesian Platform, as the BIGSEES Selection of Earthquakes covers the territory of Romania, plus ca. 100 km of neighbouring areas, which includes the Moesian Platform in northern Bulgaria. The BIGSEES Selection of Earthquakes Catalogue was compiled by the National Institute for Earth's Physics (NIEP) within their BIGSEES project and includes recordings for the time interval 984–August 2016, moment magnitude (Mw) $\geq$ 2.8 earthquakes.

A large number of seismicity maps at various time intervals and various depth intervals as well as in-depth seismicity graphs have been built, aiming to depict seismicity trends and interpret active faults or active fault segments within the Moesian Platform. The seismicity data analysis showed that the Moesian Platform, although considered a "stable" tectonic unit of the Carpathians and Balkans foreland, is still a place of active seismicity, with some very strong historical earthquake recordings.

We considered the seismic activity within the Moesian Platform to represent the expression of its contemporary geodynamics, the earthquake occurrences on the specific trending being an indicator of active faulting.

The study of the crustal movements started in Romania during the mid-1960s, being based on high-precision geodetic levelling measurements, performed on the territory of the whole country, published vertical crustal movements maps, e.g., [74–78] illustrating effects of regional active neotectonic processes.

Precise positioning using GNSS technology offers highly precise measurements of both horizontal and vertical positioning, often achieving accuracy at the millimetre level. This exceptional precision is essential for the detection and comprehensive assessment of ongoing crustal deformations—a defining characteristic of neotectonics. The recent establishment of extensive global, regional, and local networks of permanent GNSS stations has enabled continuous monitoring of the Earth's crust's horizontal and vertical movements at an unprecedented level of detail. This has revealed previously unknown modes of deformation, such as seasonal deformations with very long wavelengths [79], the Earth's elastic response to variations in atmospheric load [80], oceanic load [81], or hydrological load [82], as well as episodic tremors and slips in the Cascadia subduction zone [83,84].

Within the framework of the Central European GPS Geodynamic Reference Network (CEGRN) activities [85,86], GPS campaigns were carried out from 1994 to 2006 involving both permanent and epoch stations across Central Europe. Subsequent to this, a systematic reanalysis of these campaigns, along with additional data collected through the EU-funded CERGOP and CERGOP-2 projects [87–89], has unlocked the potential of GPS data for advancing our understanding of the regional geodynamics in the studied area.

3. Results

3.1. Geological Observations

The surface geology and the geological processes that cause tectonic uplifting and subsidence are forming the framework for the surface processes (i.e., erosion, transport, accumulation) to shape the present surface topography. When analysing the surface geology of the Moesian Platform (see Figure 3), the geological map 1:1,000,000 [90] shows that the western part of the Moesian Platform in Romania is largely covered by Middle Pleistocene sedimentary formations, while the eastern part of the Moesian Platform in Romania is covered by Late Pleistocene sedimentary formations. A boundary (blue dotted line in Figure 3) trending NW–SE along the Teleorman River, continues W–E along the Argeş

River, separating the western Middle Pleistocene area from the eastern Late Pleistocene area.

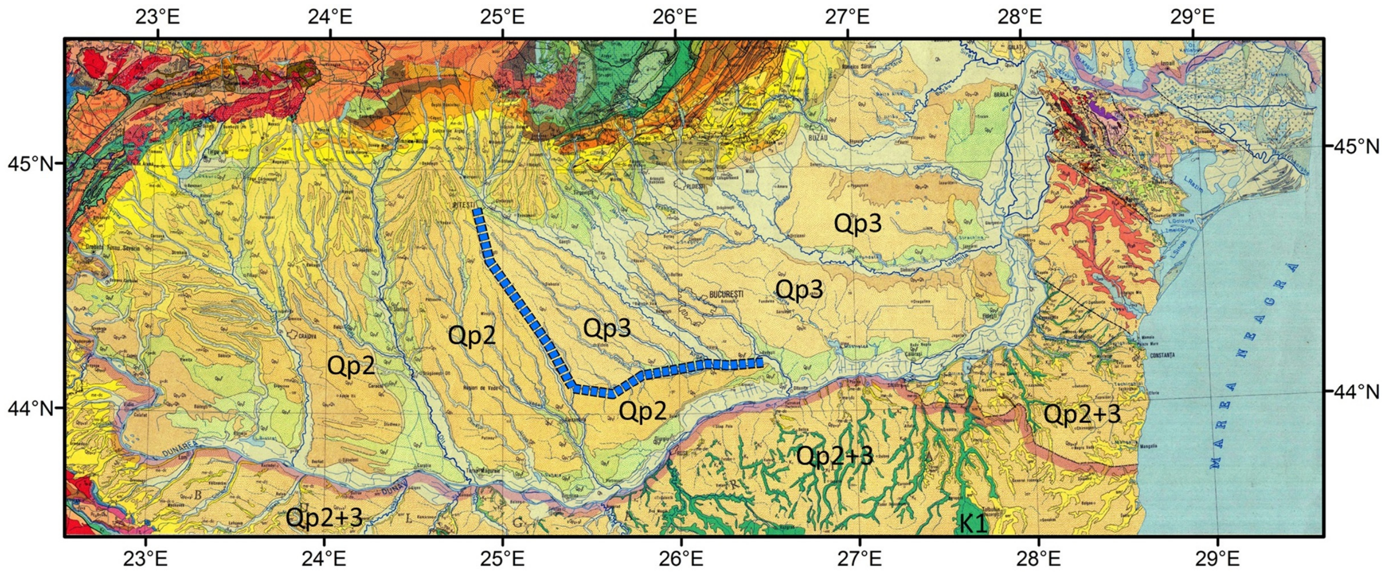

Figure 3. The surface geology as observed on the geological map 1:1,000,000 of the Moesian Platform (detail from [90], modified). Blue line = geological surface boundary, which separates the western Middle Pleistocene (Qp2) area from the eastern Late Pleistocene (Qp3) area in the Moesian Platform, north of the Danube River. Qp2+3 = Middle & Late Pleistocene. K1 = Early Cretaceous.

South of the Danube River, the Moesian Platform in Bulgaria is covered by undifferentiated Middle and Late Pleistocene sedimentary formations. In the central part of the Moesian Platform in Bulgaria, large outcrops of Lower Cretaceous massive carbonates are exposed along the rivers, while in the eastern part of the Moesian Platform in Bulgaria, large outcrops of Sarmatian limestones are exposed along the rivers and along the Black Sea coastline.

3.2. Geomorphological Observations

The geomorphological characteristics of a region could be useful clues for understanding the ongoing tectonic processes. Analysing the elevation and morphology changes across landscapes may help identify areas experiencing vertical movement due to tectonics. Tectonic movements can influence the way rivers flow and shape their courses. Sudden changes in river direction, elevation drops, or river captures (one river diverting the flow of another) may indicate tectonic events.

Within the Moesian Platform, typical elevations range between 0 and 300 m. The highest point is Tarnov Dyal (502 m altitude) on the Shumen Plateau, in Bulgaria. The lowest point (10 m altitude) is on the lower Siret River valley, in Romania, where a large confluence area was formed due to active subsidence.

North of the Danube River, in Romania, the topography of the Moesian Platform is characterised by elevations descending from west and north toward south, east, and northeast. Plains are the typical geomorphological features, with large valleys.

South of the Danube River, the Moesian Platform in Bulgaria is characterised by higher elevations than the Moesian Platform in Romania (Figure 4). Within the Bulgarian Moesian Platform, the altitude rises from west to east. Hills and plateaus are the typical geomorphological features, with steep meandering valleys (e.g., Yantra, Russenski Lom). The Bulgarian riverbank of the Danube River is steep, presenting slopes of 50–200 m, higher than the Romanian riverbank [91].

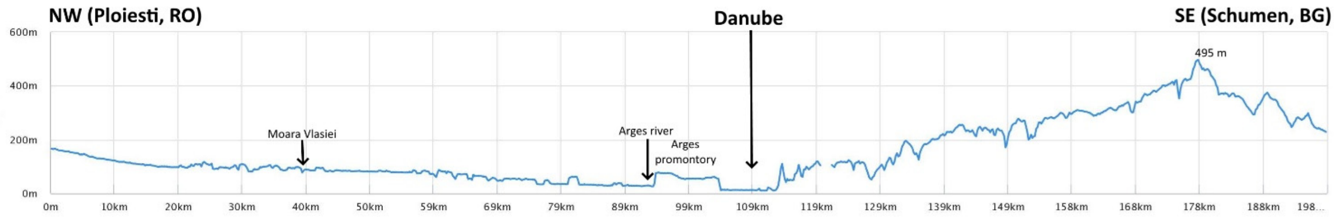

(**a**)

(**b**)

Figure 4. (**a**). NW (Ploieşti, RO)–SE (Schumen, BG) topography profile across the central part of the Moesian Platform (built on [92]). North of the Danube River, elevations are descending from NW (Ploieşti, ca. 180 m) toward SE (the Danube River, ca. 20 m). The Argeş Promontory appears as a distinct geomorphological feature (ca. 85 m maximum altitude). South of the Danube River, the Moesian Platform in Bulgaria is characterised by higher elevations (495 m at Shumen, BG) than the Moesian Platform in Romania. (**b**). Location of the topography profile.

In the southern part of the Moesian Platform in Romania, between the Argeş and Danube rivers, an elevated geomorphological feature is easily observed (Figures 4 and 5), which is named by the local inhabitants as "hill". Delineated to the north and to the east by the steep slopes of the Argeş River valley and to the south by the steep slopes of the Danube River valley, this promontory-looking area is distinct from the neighbouring flat relief of the Romanian plain.

Within the Argeş Promontory, an intriguing outcrop displaying a filled fault cutting and displacing the Upper Pliocene-Quaternary sedimentary formations was observed by Stanciu [11] in the vicinity of Crivăţ locality, Călăraşi county (Figures 6–8), during several field works carried out during 2019–2023. We named this fault the Crivăț Fault [11,63,93].

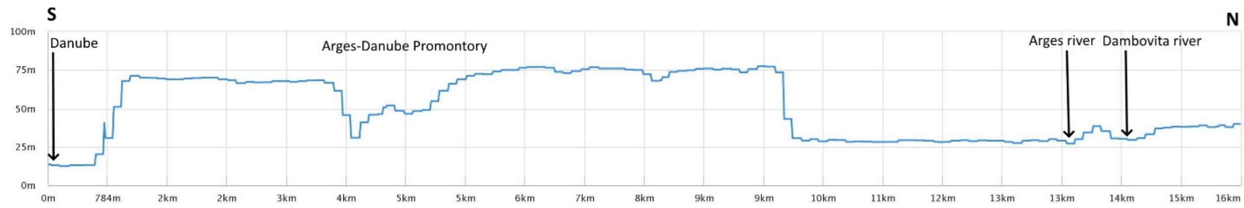

(**a**)

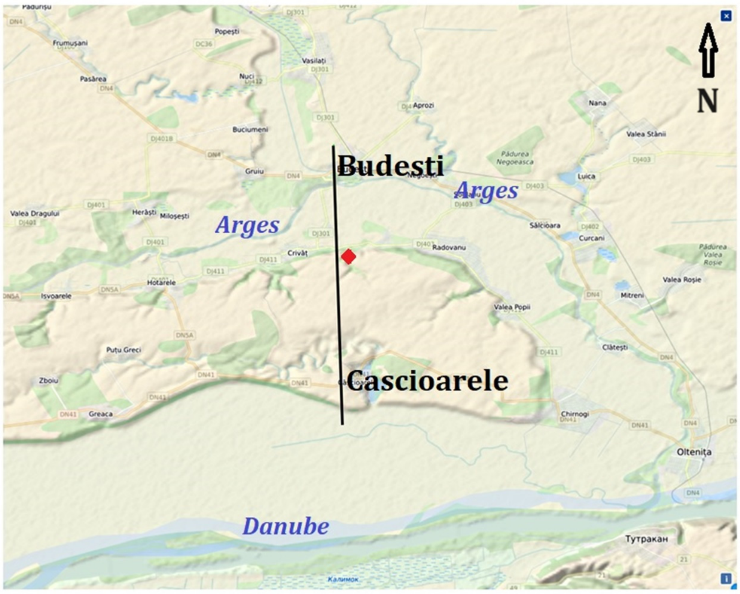

(**b**)

Figure 5. (**a**). N–S topography profile across the Argeş Promontory (built on [92]) (modified from [11,93]) (**b**). Location of the topography profile. Red rhomb marks the position of the observed Crivăt Fault outcrop.

Figure 6. Outcrop showing the newly discovered Crivăț Fault, cutting and displacing the Upper Pliocene-Quaternary sedimentary formations of the Argeş Promontory (Crivăţ locality, Călăraşi county), 2019 field works.

Figure 7. Details of the outcropping Crivat Fault in Upper Pliocene-Quaternary sedimentary formations [11]. Argeş Promontory (Crivăţ locality, Călăraşi county), 2019 field works.

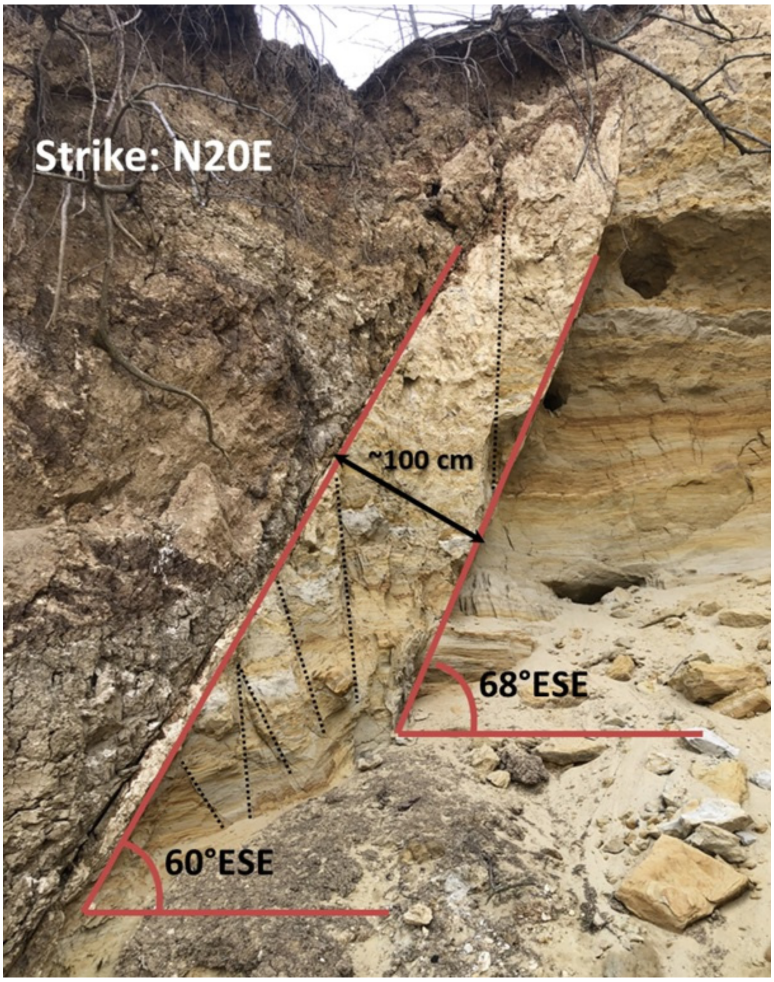

Figure 8. Observations on the Crivăţ Fault outcrop, 2022 field works. Excavations performed by local inhabitants strongly affected the outcrop. The NNE–SSW-trending Crivăţ Fault separates a

downlifted SSE compartment of outcropping Quaternary loess and soil deposits, from an uplifted NNW compartment of outcropping Upper Pliocene sand deposits of probably Romanian geological age. Black dashed lines = observed fault filling fractures.

The NNE–SSW-trending fault, characterized as a normal fault, is separating a downlifted SSE compartment of outcropping Quaternary loess and soil deposits, from an uplifted NNW compartment of outcropping cross-bedded Upper Pliocene sediments, represented by sand deposits of probably Romanian geological age [11,63,93]. The tectonic feature is a sand-filled fault, ca. 100 cm wide (Figure 8). Its apparent dipping angle varies from 60° ESE to 68° ESE.

On the opposite side of the Crivăţ Fault's uplifted compartment outcrop, two E–W parallel normal faults display a 5–13 cm jump in the sand deposits, as may be observed in Figure 9a. Their apparent dipping angle is ca 70° NNW. Spring emergences have been also observed in the fault outcrop's close vicinity (Figure 9b).

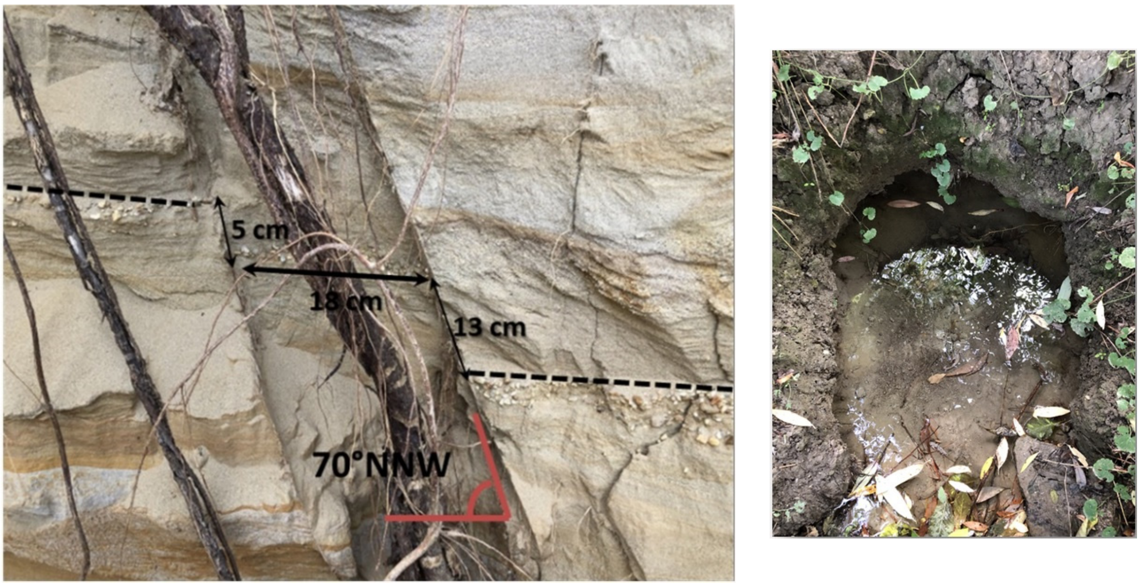

(**a**) (**b**)

Figure 9. Observations on the Crivăţ Fault outcrop, 2022 field works: (**a**)—two E–W parallel normal faults, cutting the Romanian sands; (**b**)—spring emergences observed in the Crivăţ Fault outcrop area.

Considering that rivers are largely influenced by active tectonics (river networks being sensitive to both faulting and regional surface deformation [94]), the Moesian Platform rivers' network (Figure 10) analysis emphasized several interesting aspects (also discussed in [93]):

1. The Danube River flows from W to E through the Moesian Platform, delineating the northern (Romanian) and southern (Bulgarian) parts of the Moesian Platform, as it serves as a natural boundary between Romania and Bulgaria. It acts as an axis between the main rivers of the Romanian Moesian Platform, which are trending NW–SE, and the main rivers of the Bulgarian Moesian Platform, which are trending SW–NE, towards the Romanian rivers' points of drainage.
2. The main rivers draining within the Romanian Moesian Platform run nearly perpendicular to the Carpathians, trending NW–SE in Western Moesia until they flow into the Danube River, while in Eastern Moesia the rivers turn eastward until they flow into the Danube River, and some of them turn north-eastward until they flow into the Siret River.
3. Fielitz and Seghedi [95] observed that the river network in the Romanian Moesian Platform changed from predominantly braided river channels in Western Moesia to predominantly and often extremely meandering river channels in Eastern Moesia,

due to a higher river gradient in Western Moesia vs. a lower river gradient and a finer-grained bedload in the Eastern Moesia, as well as due to the subsidence affecting the Focşani Depression.

4. Mostiştea is the easternmost river in the Moesian Platform flowing in the NW–SE direction. Overall, its right (western) bank is slightly elevated than the eastern one. However, in the Mostiştea lake area, the right (western) bank shows a more than 20 m steep slope of leoss-paleosoil sequences [96,97], overlying fluvio-lacustrine sediments, which contain mammal fossils of Pleistocene age [96].
5. On the western bank of the Mostiştea lake (Sultana locality, Călăraşi county), local NE–SW-trending faults affecting the outcropping sedimentary layers have been observed during field works in 2020 [11].
6. Western Moesia's river network is denser than Eastern Moesia's river network.
7. A transition zone from Western Moesia's river drainage to Eastern Moesia's river drainage, between the Teleorman and Mostiştea rivers, refers to the Argeş drainage basin. The Argeş River and all its tributaries within the Moesian Platform have NW–SE courses, which suddenly end south of Bucharest on a sharp W–E change of flow direction. The morphology of the W–E Argeş River valley displays a southern steep bank, ca 15 m in height, which separates a southern uplifted, hilly geomorphology compartment (i.e., the Argeş Promontory) from a northern, flat geomorphology compartment. The observed W–E uplifted Argeş Promontory acts as a barrier for the Argeş River and its tributaries and displaces the Argeş River course eastward by ca. 25 km. Right before the point where the Dâmboviţa River flows into the Argeş River, a ca. 3 km north-eastward displacement of the Argeş River is also to be observed. Meandering palaeo-valleys of the Argeş River are still to be observed in this area on remote sensing imagery data, including Google Earth. After the point where the Dâmboviţa river flows into the Argeş River and the Argeş Promontory ends, the Argeş River returns to its NW–SE course and flows into the Danube River.

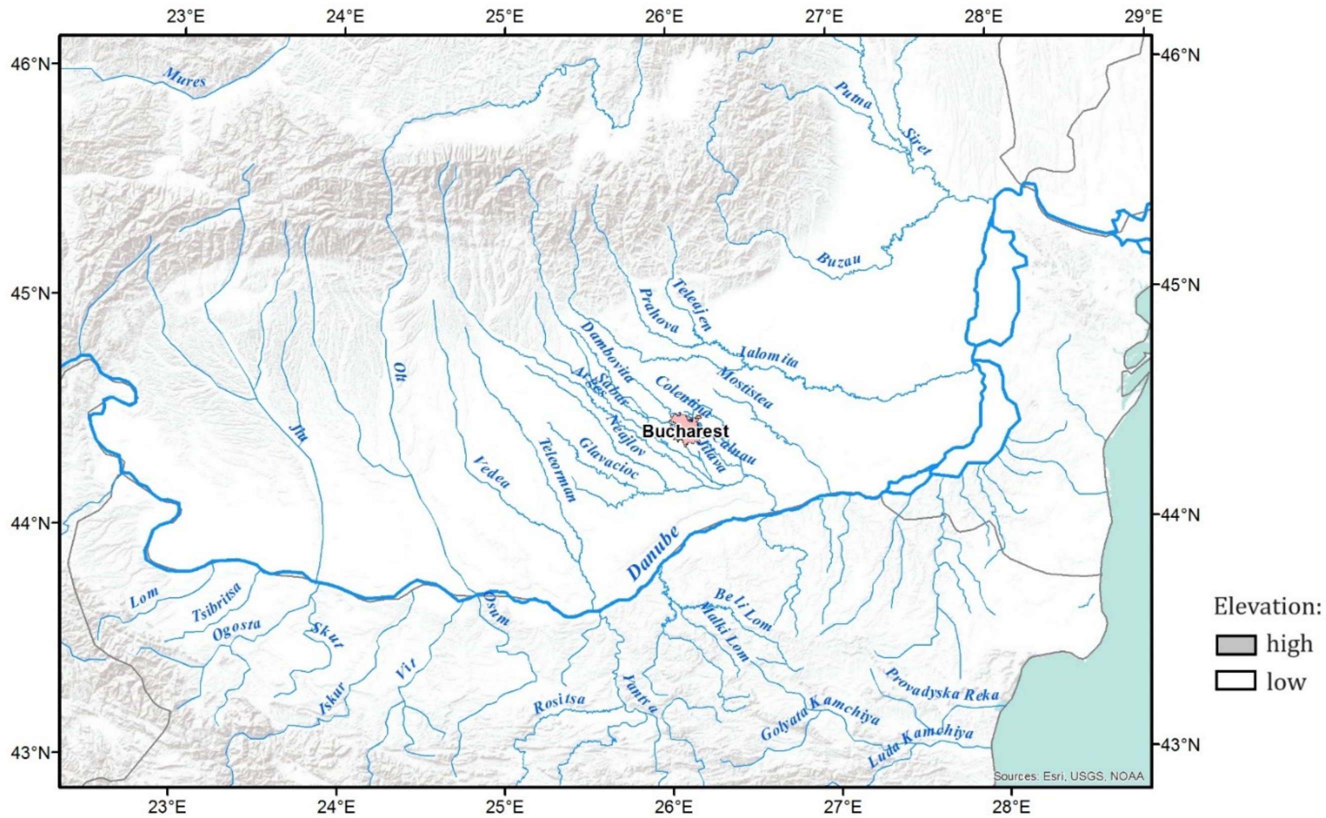

Figure 10. Network of rivers in the Moesian Platform [11,93].

3.3. Seismicity within the Argeş Promontory Area

Studying the distribution and intensity of earthquakes in a region can provide direct evidence of ongoing tectonic processes. The relationship between seismic activity and surface features can help understand the geological forces at play. An NW–SE High Seismicity Boundary was interpreted across the Moesian Platform [57,59], separating an eastern high seismicity compartment of the Moesian Platform from a western, low seismicity compartment. The lack of seismicity within the Argeş Promontory appears as an eastward indent of the High Seismicity Boundary, as illustrated in Figure 11.

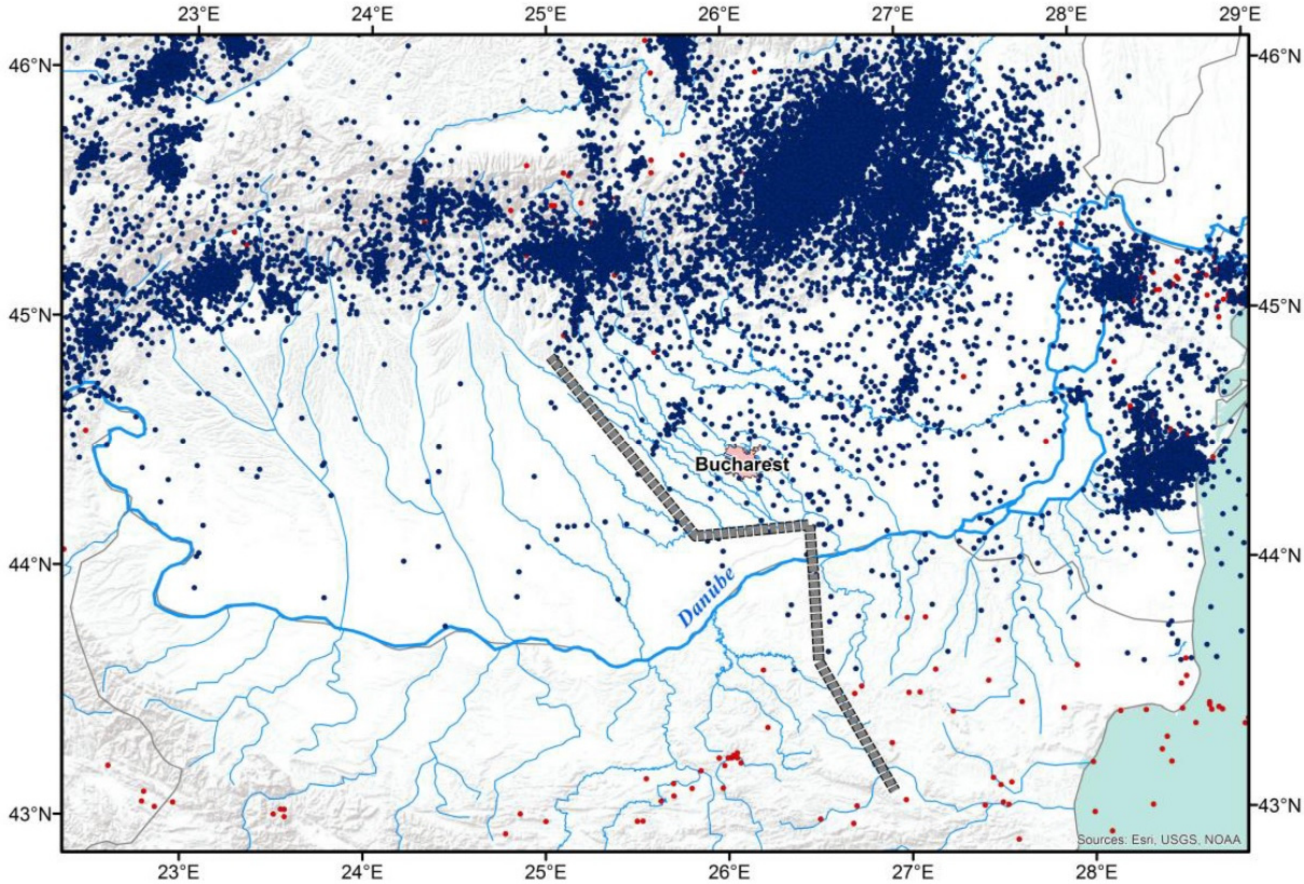

Figure 11. The seismicity of the Moesian Platform and the interpreted High Seismicity Boundary—grey line (modified after [59]). Seismological data from ROMPLUS ([64], dark blue dots) and BIGSEES ([65], red dots) earthquake catalogues.

A W–E in-depth crustal seismicity section (Figure 12), built on the 44.1 N–44.2 N wide latitude sector, in the Moesian Platform along the Argeş Promontory eastern part, illustrates an almost vertical succession of seismic events observed at 26.6 N longitude up to 10 km depth, which may represent an active fault. Its in-depth change in inclination between 10 and 15 km may be due to a past compressional regime whose intensity was variable with depth.

Detailed seismicity data analysis [11,57] shows that the Moesian Platform, although considered a "stable" tectonic unit of the Carpathians and Balkans foreland, is still a place of active seismicity. The seismic activity within the Moesian Platform represents the expression of its contemporary geodynamics, the earthquake occurrences on the specific trending being considered an indicator of active faulting.

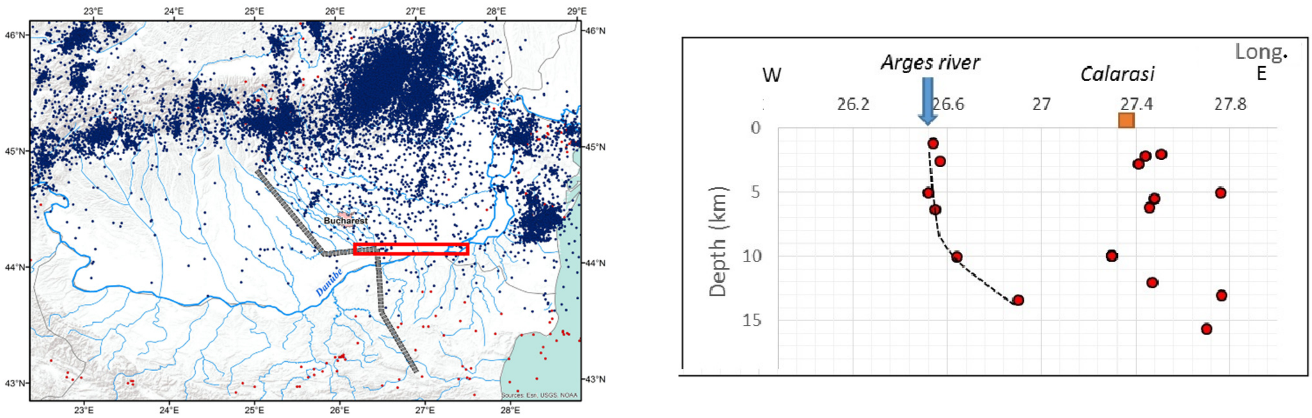

(**a**) (**b**)

Figure 12. (**a**) Location of the seismicity section (red rectangle) on the seismicity map of the Moesian Platform from Figure 11. (**b**) W–E in-depth crustal seismicity section in the Moesian Platform, along the Argeş Promontory eastern part, on a 44.1 N–44.2 N wide latitude sector (modified from [57]). Red points = earthquake hypocenters, ROMPLUS Earthquake Catalogue data [64]. Black dashed line = interpreted fault at the eastern end of the Argeş Promontory. Orange square = representation of Călărași city location along the profile.

3.4. Satellite Geodetic Data Analysis

When addressing the Moesian Platform, the present-day geodynamic processes as illustrated by GPS monitoring results [88,89,98–101] show a south-eastward displacement of the East Carpathians Bend Zone and its foreland and southward displacement of the central part of the Moesian Platform in Romania, just north of the Argeş River in our study area.

The 1997–2004 GPS research campaigns on crustal deformation in Romania based on GPS monitoring in the South-Eastern Carpathians and their foreland [98,99] show two main movement directions in the Moesian Platform, separated by the Intramoesian Fault: a SE-oriented horizontal displacement in Eastern Moesia (ca. 2.5 mm/yr) and a south-oriented motion in Western Moesia (1–2 mm/yr), all relative to stable Eurasia (Figure 13, Romanian territory).

Results of the GPS measurements carried out on 1996, 1997, 1998, and 2000 campaigns in Bulgaria, presented and interpreted by Kotzev et al. [102,103], emphasized a north-eastward displacement of the central Bulgarian Moesian Platform, with horizontal velocities of 3 mm/yr at the KAIL station (azimuth 40° E) and 2.9 mm/yr at the GABR station (azimuth 56° E) (Figure 13, Bulgarian territory). The horizontal movements were calculated with respect to the fixed Eurasia plate.

A generalized picture of horizontal movements for Central Europe and the Balkan Peninsula shows a clockwise rotation with the centre in Serbia and south-oriented and south-east-oriented velocity vectors for Romania and Bulgaria, as opposed to a counter-clockwise rotation in the Eastern Mediterranean region, observed by the GPS data [88,89,101,104–110].

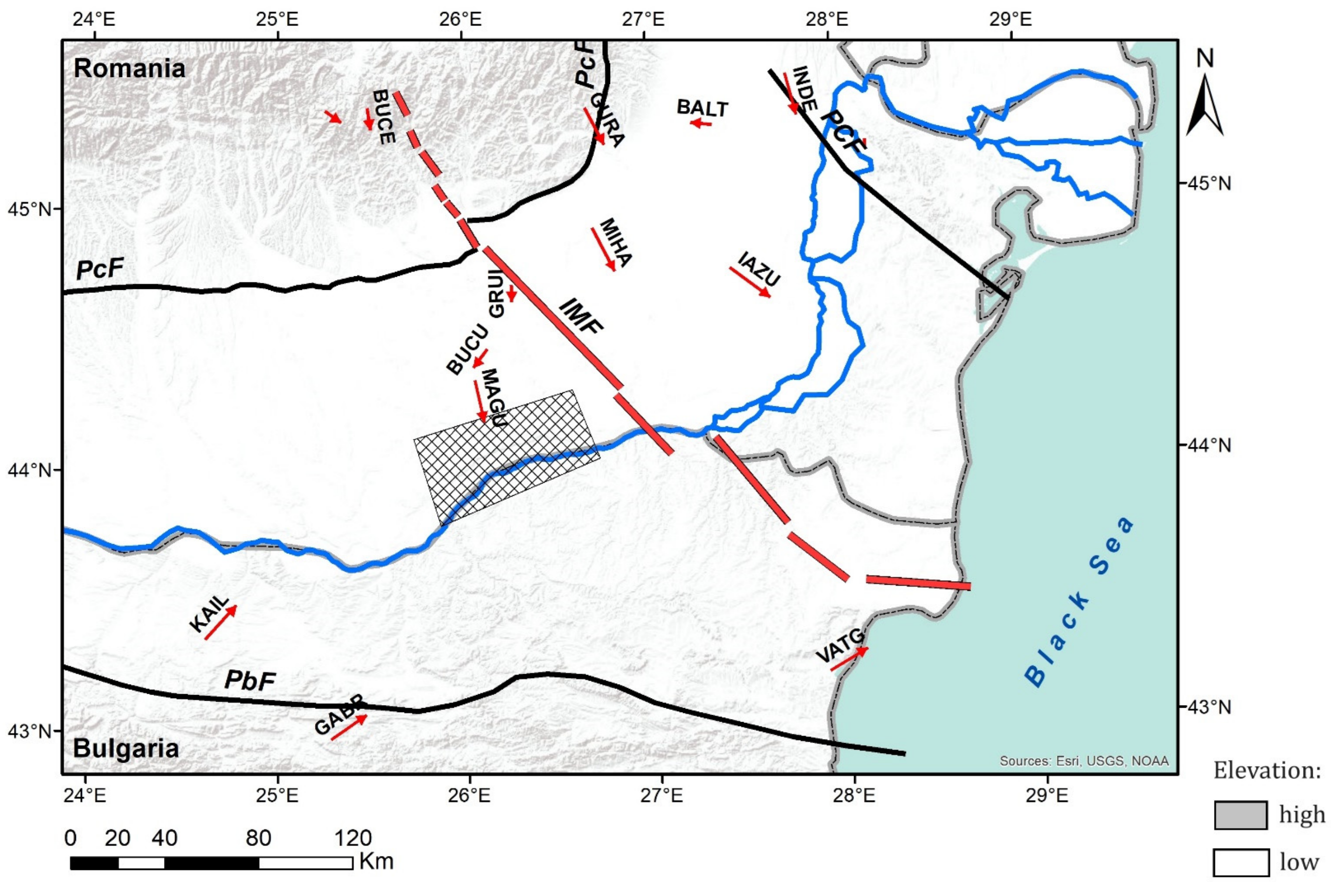

Figure 13. Horizontal crustal movements in the Moesian Platform as resulted from GPS monitoring results. The red arrows indicate the measured GPS vectors with respect to the fixed Eurasia plate (compiled from [99,102,103]). Thick black lines = Moesian Platform delineating faults (PcF = Pericarpathian Fault; PbF = Prebalkan Fault; PCF = Peceneaga-Camena Fault). Thick red line = Intramoesian Fault (IMF). Blue lines = the Danube River. Crosshatched polygon = the Argeș Promontory area.

4. Discussion

Regional geodynamic models and recent space geodetic measurements indicate that the northward-moving African and Arabian plates collide with the Eurasian plate, e.g., [111–113]. The faster 23–35 mm/y opening of the southern Atlantic Ocean, as opposed to the slower 18–23 mm/y opening of the northern Atlantic Ocean [112] caused the counter-clockwise rotation of the Africa (Nubia) plate and its NNE displacement towards the Eurasia plate. Taking the Africa plate as a reference, Bird's tectonic plates geodynamic model [113] indicates an NNW–SSE 11 mm/y movement of the Eurasia plate, which is opposed to the 15 mm/y SSE–NNW movement of the Arabian plate, causing a relative displacement of Anatolia plate to ENE by 21 mm/y and a 37 mm/y SSV relative displacement of the Aegean plate toward the Africa plate. As a consequence, in the Mediterranean Sea basin and its eastern prolongation (Black Sea basin), a series of complex geological phenomena occurred, such as subduction, continental collision, spreading, strike-slip faulting, etc.

Kotzev et al.'s [102,103] results from GPS measurements carried out in Bulgaria advocate for displacements toward the northeast in the central part of the Moesian Platform, in the Danube and Argeş Promontory area.

The regional tectonic compression resulted from the southward displacement of the central part of the Moesian Platform in Romania, just north of the Argeş River in our study area versus the north-eastward horizontal displacement in northern Bulgaria, creating or re-activating the E–W fault system, determining the build-up of the Argeş Promontory suite of crustal shortening, locally influencing the rivers course. This tectonic regime may (re-)activate faults from the NE–SW fault system, developed as strike-slip faults in the Vrancea seismic zone in Romania.

North of the Danube River, the west-east change in the surface geology from the Middle Pleistocene to Late Pleistocene shown in Figure 3 may be interpreted as due to uplifting in the western part of the Moesian Platform, west of the NW–SE blue line and south of the W–E blue line in the Argeş Promontory, versus significant subsidence processes in its eastern part (sustained also by high-precision geodetic levelling measurements results [74–78]). South of the Danube River, the Lower Cretaceous and Sarmatian limestone large outcrops exposed along the rivers suggest uplifting in the northern central and north-eastern parts of the Moesian Platform in Bulgaria, the results of the geodetic measurements carried out here [114], showing positive crustal movements of 2–3 mm/year in the Ruse area (Bulgaria), just south of the Argeş Promontory and the Danube River. We consider that the uplift was more intense in the northern central part of Bulgaria, where Lower Cretaceous massive carbonates are exposed along the rivers, as compared to the north-eastern part, where Sarmatian limestones are exposed along the rivers and on the Black Sea coastline.

A High Seismicity Boundary was interpreted along the Argeş River (published and discussed by the authors [59]), separating an eastern high-seismicity compartment from a western low-seismicity compartment of the Moesian Platform, while the Argeş Promontory shows no significant seismicity, as illustrated in Figure 11.

The rise of the Argeş Promontory has been a gradual process, shown by successive palaeo-beds of the Argeş River course while displacing eastward, toward the confluence with the Dâmbovița River. This is still to be observed on remote sensing imagery data.

The E–W-trending Argeş River, delineating the Argeş Promontory by high escarpments, as well as the course of the River Danube are controlled by the E–W fault system, largely developed in the western part of the Moesian Platform in Romania and in the central and north-eastern parts of Moesian Platform in Bulgaria [1,2,10,11,60] (Figure 2).

The Crivăț Fault of the Argeş Promontory has been possibly active during the Upper Pliocene–Lower Quaternary, due to the regional tectonic regime. The Crivăț Fault fill is represented, within the available outcrop, by the sand of the Romanian age. However, since the Quaternary loess formation is cut and vertically displaced by the Crivăț Fault, it suggests that the fault has been active or reactivated during the Quaternary. The sand of the Romanian age did flow downward into the void created by the open normal fault. The Quaternary loess formation was more compact and less mobile than the sand and did not contribute to the fault filling.

The Crivăț Fault, located at ca. 30 km SE of Bucharest city, is not presently seismically active, as observed from seismicity data analysis.

5. Conclusions

During field research carried out in the southern part of the Moesian Platform in Romania, an elevated and W–E promontory-looking geomorphological feature has been observed: the Arges Promontory.

Within the Argeş Promontory, a filled fault cutting and displacing the Upper Pliocene-Quaternary sedimentary formations was observed in the vicinity of Crivăţ locality. The NNE–SSW-trending fault, characterized as a normal fault, is separating a downlifted SSE compartment of outcropping Quaternary loess and soil deposits from an uplifted NNW compartment of outcropping cross-bedded Upper Pliocene sediments, represented by sand deposits probably from the Romanian geological age. Since the Quaternary loess formation is cut and vertically displaced by the Crivăț Fault, the fault has been active or reactivated during the Quaternary.

We consider the regional tectonic regime resulted from the southward displacement of the central part of the Moesian Platform in Romania, just north of Argeş River study area, versus the north-eastward horizontal displacement in northern Bulgaria, creating or re-activating the E-W fault system, determined the build-up of the Argeş Promontory suite of an upward extrusion of the geological formations of the Argeș Promontory and a local eastward lateral escape, of ca. 25 km, of the uplifted structure, taking into account the Argeș River course displacement. The rise of the Argeş Promontory has been a gradual process, shown by successive palaeo-beds of the Argeş River course while displacing eastward, toward the confluence with the Dâmbovița River, observed on remote sensing imagery data.

Author Contributions: Conceptualization, I.S. and D.I.; methodology, I.S. and D.I.; field works, I.S.; investigation, I.S. and D.I.; resources, I.S.; data curation, I.S.; writing—original draft preparation, I.S. and D.I.; writing—review and editing, I.S. and D.I.; visualization, I.S. All authors have read and agreed to the published version of the manuscript.

Funding: This research received no external funding.

Data Availability Statement: The ROMPLUS earthquake data presented in this study are openly available in Mendeley Data at [10.17632/tdfb4fgghy.2], reference number [64]. The BIGSEES earthquake data presented in this study are openly available online at http://infp.infp.ro/bigsees/Results.html, reference number [65]. If any other questions on the presented data, please address the corresponding author.

Conflicts of Interest: The authors declare no conflict of interest.

References

1. Săndulescu, M. *Geotectonica României*; Editura Tehnică: Bucharest, Romania, 1984; p. 336.
2. Visarion, M.; Săndulescu, M.; Stănică, D.; Veliciu, S. Contributions à la connaissance de la structure profonde de la plateforme Moésienne en Roumanie. *Stud. Teh. Econ.-Geofiz.* **1988**, *15*, 68–92.
3. Săndulescu, M. The Rumanian Foreland. In *Tectonics of the Carpathian Balkan Regions, Platforms of the Foreland*; Geological Institute of Dionyz Stur: Bratislava, Slovakia, 1974; pp. 446–449.
4. Paraschiv, D. *Platforma Moesică și Zăcămintele ei de Hidrocarburi*; Editura Academiei Române: Bucharest, Romania, 1979; p. 196.
5. Tărăpoancă, M.; Bertotti, G.; Maţenco, L.; Dinu, C.; Cloetingh, S.A.P.L. Architecture of the Focşani Depression: A 13 km deep basin in the Carpathians bend zone (Romania). *Tectonics* **2003**, *22*, 1074. [CrossRef]
6. Seghedi, A.; Berza, T.; Iancu, V.; Mărunţiu, M.; Oaie, G. Neoproterozoic terranes in the Moesian basement and in the Alpine Danubian nappes of the South Carpathians. *Geol. Belg.* **2005**, *84*, 4–19.
7. Seghedi, A.; Vaida, M.; Iordan, M.; Verniers, J. Paleozoic evolution of the Romanian part of the Moesian Platform: An overview. *Geol. Belg.* **2005**, *84*, 99–120.
8. Boncev, E. Moesian Platform. In *Tectonics of the Carpathian Balkan Regions, Platforms of the Foreland*; Geological Institute of Dionyz Stur: Bratislava, Slovakia, 1974; pp. 449–453.
9. Zagorchev, I. Geomorphological zonation of Bulgaria. Principles and state of the art. *Compt. Rend. Acad. Bul. Sci.* **2009**, *62*, 981–992.
10. Tari, G.; Dicea, O.; Faulkerson, J.; Georgiev, G.; Popov, S.; Ştefănescu, M.; Weir, G. Cimmerian and Alpine stratigraphy and structural evolution of the Moesian Platform. In *Regional and Petroleum Geology of the Black Sea and Surrounding Regions*; Robinson, A.G., Ed.; American Association of Petroleum Geologists: Tulsa, OK, USA, 1997; Volume 68, pp. 63–90.
11. Stanciu, I.M. Intramoesian Fault: Geophysical Detection and Regional Active (Neo)Tectonics and Geodynamics. Ph.D. Thesis, Doctoral School of Geology, Faculty of Geology and Geophysics, University of Bucharest, Bucharest, Romania, 2020.
12. Relief Map. Available online: https://maps-for-free.com/ (accessed on 5 January 2021).
13. Burchfiel, B.C. *Geology of Romania*; Geological Society of America: Boulder, CO, USA, 1976; Volume 158, pp. 1–82. [CrossRef]
14. Ziegler, P.A. Geodynamic model for the Palaeozoic crustal consolidation of W. and C. Europe. *Tectonophysics* **1986**, *126*, 303–328. [CrossRef]
15. Matte, P.; Maluski, H.; Railich, P.; Franke, W. Terrane boundaries in the Bohemian Massif: Result of large scale Variscan shearing. *Tectonophysics* **1990**, *177*, 151–170. [CrossRef]
16. Kalvoda, J. Upper Devonian-Lower Carboniferous foraminiferal palaeobiogeography and Perigondwana terranes at the Baltica-Gondwana interface. *Geol. Carpathica* **2001**, *52*, 205–215.
17. Yanev, S. Gondwana Paleozoic terranes in the Alpine collage system of the Balkans. *Himal. Geol.* **1993**, *4*, 257–270.
18. Yanev, S. *Paleozoic Migration of Terranes from the Basement of the Eastern Part of the Balkan Peninsula from Peri-Gondwana to Laurussia*; Special Publication 3; Turkish Association Petroleum Geologists: Ankara, Turkey, 1997; pp. 89–100.
19. Yanev, S. Palaeozoic terranes of the Balkan Peninsula in the framework of Pangea assembly. *Palaeogeogr. Palaeoclimatol. Palaeoecol.* **2000**, *161*, 151–177. [CrossRef]
20. Yanev, S.; Boncheva, I. Contribution to the Paleozoic evolution of the recent Moesian platform. *Geol. Balc.* **1995**, *25*, 3–23. [CrossRef]

21. Yanev, S.; Boncheva, I. *New Data on the Collision between Peri-Gondwana Moesian Terrane and Dobrudja Periphery of Paleo Europe*; Special Publication 3; Turkish Association Petroleum Geologists: Ankara, Turkey, 1997; pp. 118–132.
22. von Raumer, J.V.; Stampfli, G.M.; Borel, G.; Bussy, F. Organization of pre-Variscan basement areas at the north-Gondwanan margin. *Int. J. Earth Sci.* **2002**, *91*, 35–52. [CrossRef]
23. von Raumer, J.V.; Stampfli, G.M.; Bussy, F. Gondwana-derived microcontinents—The constituents of the Variscan and Alpine collisional orogens. *Tectonophysics* **2003**, *365*, 7–22. [CrossRef]
24. Deroin, J.P.; Bonin, B. Late Variscan tectonomagmatic activity in Western Europe and surrounding areas: The Mid-Permian episode. *Ital. J. Geosci.* **2003**, *2*, 169–184.
25. Żelaźniewicz, A.; Marheine, D.; Oberc-Dziedzic, T. A Late Tournaisian synmetamorphic folding and thrusting event in the eastern Variscan foreland: 40 Ar/39 Ar evidence from the phyllites of the Wolsztyn–Leszno High, western Poland. *Int. J. Earth Sci.* **2003**, *92*, 185–194. Available online: https://link.springer.com/content/pdf/10.1007%2Fs00531-002-0306-7.pdf (accessed on 1 May 2020). [CrossRef]
26. Żelaźniewicz, A.; Oberc-Dziedzic, T.; Fanning, C.M. The Trans-European Suture Zone: Origin and tectonomagmatic events in late Variscan times. In Proceedings of the 35th International Geological Congress, Cape Town, South Africa, 27 August–4 September 2016; p. 2481. Available online: https://www.americangeosciences.org/sites/default/files/igc/2481.pdf (accessed on 1 May 2020).
27. Yanev, S.; Lakova, I.; Boncheva, I.; Sachanski, V. The Moesian and Balkan terranes in Bulgaria: Palaeozoic basin development, palaeogeopgraphy and tectonic evolution. *Geol. Belg.* **2005**, *84*, 185–192.
28. Oczlon, M.S.; Seghedi, A.; Carrigan, C.W. Avalonian and Baltican terranes in the Moesian Platform (southern Europe, Romania, and Bulgaria) in the context of Caledonian terranes along the southwestern margin of the East European craton. In *The Evolution of the Rheic Ocean: From Avalonian-Cadomian Active Margin to Alleghenian-Variscan Collision*; Special Paper 423; Linnemann, U., Nance, R.D., Kraft, P., Zulauf, G., Eds.; Geological Society of America: Boulder, CO, USA, 2007; pp. 375–400. [CrossRef]
29. Săndulescu, M. The Geotectonic framework of a peculiar seismogenic area—The Vrancea seismic zone (Romanian Carpathians). *Proc. Rom. Acad. Ser. B* **2009**, *2–3*, 151–157. Available online: https://acad.ro/sectii2002/proceedingsChemistry/doc2009-23/art10Sandulescu.pdf (accessed on 10 September 2019).
30. Artemieva, I.M.; Thybo, H. EUNAseis: A seismic model for Moho and crustal structure in Europe, Greenland, and the North Atlantic region. *Tectonophysics* **2013**, *609*, 97–153. [CrossRef]
31. Winchester, J.A.; Pharaoh, T.C.; Verniers, J. Palaeozoic amalgamation of Central Europe: An introduction and synthesis of new results from recent geological and geophysical investigations. In *Palaeozoic Amalgamation of Central Europe*; Special Publications; Winchester, J.A., Pharaoh, T.C., Verniers, J., Eds.; Geological Society: London, UK, 2002; Volume 201, pp. 1–18.
32. Stille, H. Der tektonische Werdegang der Karpaten. *Beih. Z. Geol. Jahrb.* **1953**, *8*, 1–239.
33. Berza, T.; Constantinescu, E.; Vlad, Ş.N. Upper Cretaceous magmatic series and associated mineralisation in the Carpathian-Balkan Orogen. *Res. Geol.* **1998**, *48*, 291–306. [CrossRef]
34. Ratschbacher, L.; Linzer, H.G.; Moser, F.; Strusievicz, R.-O.; Bedelean, H.; Har, N.; Mogoş, P.A. Cretaceous to Miocene thrusting and wrenching along the central South Carpathians due to a corner effect during collision and orocline formation. *Tectonics* **1993**, *12*, 855–873. [CrossRef]
35. Linzer, H.G. Kinematics of retreating subduction along the Carpathian arc, Romania. *Geology* **1996**, *24*, 167–170. [CrossRef]
36. Hippolyte, J.C. Geodynamics of Dobrogea (Romania): New constraints on the evolution of the Tornquist-Tesseire Line, the Black Sea and the Carpathians. *Tectonophysics* **2002**, *357*, 33–53. [CrossRef]
37. Rădulescu, D.P.; Cornea, I.; Săndulescu, M.; Constantinescu, P.; Rădulescu, F.; Pompilian, A. Structure de la croûte terrestre en Roumanie—Essai d'interprétation sismiques profonds. *An. Inst. Geol. Geof.* **1976**, *50*, 5–36.
38. Rădulescu, F. Seismic models of the crustal structure in Romania. *Rev. Roum. Géol. Géophys. Géogr. Sér. Géophys.* **1988**, *32*, 13–17.
39. Răileanu, V.; Diaconescu, C.; Rădulescu, F. Characteristics of Romanian lithosphere from deep seismic reflection profiling. *Tectonophysics* **1994**, *239*, 165–185. [CrossRef]
40. Hauser, F.; Răileanu, V.; Fielitz, W.; Bălă, A.; Prodehl, C.; Polonic, G.; Schulze, A. VRANCEA99—The crustal structure beneath the southeastern Carpathians and the Moesian Platform from a seismic refraction profile in Romania. *Tectonophysics* **2001**, *340*, 233–256. [CrossRef]
41. Hauser, F.; Răileanu, V.; Fielitz, W.; Dinu, C.; Landes, M.; Bălă, A.; Prodehl, C. Seismic crustal structure between the Transylvanian Basin and the Black Sea, Romania. *Tectonophysics* **2007**, *430*, 1–25. [CrossRef]
42. Polonic, G. Structure of the crystalline basement in Romania. *Rev. Roum. Geophys.* **1996**, *40*, 57–70.
43. Paraschiv, D. *Geologia Zăcămintelor de Hidrocarburi din România*; Institutul de Geologie și Geofizică: Bucharest, Romania, 1975; p. 327.
44. Burcea, C.; Cornea, I.; Ţugui, G.; Ionescu, E.; Trîmbiţaş, M.; Georgescu, S.; Leafu, I.; Tomescu, L., II; Braşoveanu, A.; Chişcan, M.; et al. Contribuţii seismice la crearea unei imagini tectonice asupra marginii nordice a Platformei Moesice între Olt şi Buzău. *St. Cerc. Geol. Geofiz. Geogr. Ser. Geofiz.* **1965**, *3*, 129–139.
45. Burcea, C.; Cornea, I.; Ţugui, G.; Tomescu, L., II; Ionescu, E.; Trîmbiţaş, M.; Leafu, I.; Dumitrescu, V.; Braşoveanu, A.; Sipoş, V.; et al. Contribuţii ale prospecţiunii seismice la crearea unei imagini tectonice în zona centrală a Platformei Moesice. *St. Cerc. Geol. Geofiz. Geogr. Ser. Geofiz.* **1966**, *4*, 347–353.

46. Dumitrescu, I.; Săndulescu, M. Harta tectonică a României, 1:1,000,000. In *Atlasul Geologic*; Foaia Nr. 6; Geological Institute of Romania: Bucharest, Romania, 1970.
47. Cornea, I.; Polonic, G. Date privind seismicitatea şi seismotectonica părţii de est a Platformei Moesice. *Stud. Cercet. Geol. Geofiz. Geogr. Geofiz.* **1979**, *17*, 167–176.
48. Săndulescu, M.; Visarion, M. La structure des plate-formes situees dans l'avant-pays et au-dessous des nappes du flysch des Carpathes Orientales. *St. Teh. Econ. Geofiz.* **1988**, *15*, 62–67.
49. Dicea, O. The structure and hydrocarbon geology of the Romanian East Carpathians border from seismic data. *Pet. Geosci.* **1995**, *1*, 135–143. [CrossRef]
50. Matova, M. Recent geological activity along the northeastern Bulgarian Black Sea coast. *Geol. Quaterly* **2000**, *44*, 355–361. Available online: https://gq.pgi.gov.pl/article/viewFile/8109/pdf_215 (accessed on 15 September 2016).
51. Dinu, C.; Wong, H.K.; Ţămbrea, D.; Maţenco, L. Stratigraphic and structural characteristics of the Romanian Black Sea shelf. *Tectonophysics* **2005**, *410*, 417–435. [CrossRef]
52. Shanov, S.; Boycova, A.; Mitev, A. Intramoesian Fault on Bulgarian territory: Available geophysical data. In Proceedings of the 4th Congress of the Balkan Geophysical Society, Bucharest, Romania, 9 October 2005; Volume 8, pp. 56–59. [CrossRef]
53. Săndulescu, M.; Visarion, M. Crustal structure and evolution of the Carpathian-Western Black Sea areas. *First Break* **2000**, *18*, 103–108. [CrossRef]
54. Visarion, M.; Beşuţiu, L. Transcrustal faults on the Romanian territory. *St. Cerc. Geofiz.* **2001**, *39*, 15–33.
55. Ioane, D.; Diaconescu, M.; Chitea, F.; Gârbacea, G. Active Fault Systems and Their Significance for Urban Planning in Bucharest, Romania. In *Earthquake Hazard Impact and Urban Planning*; Boştenaru, D., Armaş, I., Goretti, A., Eds.; Springer: Berlin/Heidelberg, Germany, 2014; pp. 15–45.
56. Ioane, D.; Diaconescu, M.; Chitea, F.; Caragea, I. Active Fault Systems as Interpreted on Gravity and Seismicity Data in Bucharest-Vrancea Area. In Proceedings of the GEO 2014 Symposium, Bucharest, Romania, 26 April 2014.
57. Stanciu, I.M.; Ioane, D. Regional seismicity in the Moesian Platform and the Intramoesian Fault. *Geo-Eco-Marina* **2017**, *23*, 263–271.
58. Stanciu, I.M.; Ioane, D. Regional active faults as interpreted on crustal seismicity, gravity and magnetic data across the Moesian Platform and the North Dobrogean Orogen. In Proceedings of the 18th International Multidisciplinary Scientific GeoConference on Earth & Geosciences SGEM2018, Albena Resort, Bulgaria, 30 June–9 July 2018; Volume 18, pp. 939–946.
59. Stanciu, I.M.; Ioane, D. Seismicity associated to the Intramoesian Fault: Inferences from regional tectonics and geodynamics. In Proceedings of the 19th International Multidisciplinary Scientific GeoConference on Earth & Geosciences SGEM2019, Albena, Bulgaria, 28 June–7 July 2019; Volmue 19, pp. 923–930. [CrossRef]
60. Stanciu, I.; Ioane, D. Active fault systems in the Shabla region (Bulgaria) as interpreted on geophysical and seismicity data. *Rev. Roum. Geophys./Rom. Geophys. J.* **2021**, *63–64*, 3–21. [CrossRef]
61. Stanciu, I.; Ioane, D. The Moesian Platform: Structural and tectonic features interpreted on regional gravity and magnetic data. *Geo-Eco-Marina* **2021**, *27*, 183–195. [CrossRef]
62. Ioane, D.; Caragea, I. Western Boundary of East European Platform in Romania as Interpreted on Gravity and Magnetic Data. In Proceedings of the 8th Congress of the Balkan Geophysical Society, Greece, Chania, 4–8 October 2015. [CrossRef]
63. Stanciu, I.; Ioane, D. Outcrop-based analysis of a recently discovered fault offsetting Upper Pliocene-Quaternary sedimentary deposits in the Moesian Platform (Romania). In *ILP–Geoscience 2022. Book of Abstracts*; Chitea, F., Munteanu, I., Mațenco, L., Dinescu, R., Stanciu, I., Eds.; Editura Cetatea de Scaun: Târgoviște, Romania, 2022; ISBN 978-606-537-578-9.
64. Popa, M.; Chircea, A.; Dinescu, R.; Neagoe, C.; Grecu, B.; Borleanu, F. *Romanian Earthquake Catalogue (ROMPLUS 984-2022)*; Mendeley Data, V2; Institutul National de Cercetare-Dezvoltare pentru Fizica Pamantului: Ilfov County, Romania, 2022. Available online: https://doi.org/10.17632/tdfb4fgghy.2 (accessed on 30 January 2023).
65. BIGSEES Selection of Earthquakes Catalogue. Available online: http://infp.infp.ro/bigsees/Results.html (accessed on 10 December 2019).
66. EMSC Earthquake Catalogue. Available online: http://www.emsc-csem.org (accessed on 10 December 2019).
67. ISC-GEM Global Instrumental Earthquake Catalogue. Available online: http://www.isc.ac.uk/iscgem/download.php (accessed on 10 December 2019).
68. Grünthal, G.; Wahlström, R. The European-Mediterranean Earthquake Catalogue (EMEC) for the last millennium. *J. Seismol.* **2012**, *16*, 535–570. [CrossRef]
69. Shebalin, N.V.; Leydecker, G.; Mokrushina, N.G.; Tatevossian, R.E.; Erteleva, O.O.; Vassiliev, V.Y. *Earthquake Catalogue for Central and Southeastern Europe 342 BC—1990 AD*; Report No. ETNU CT 93-0087; European Commission: Brussels, Belgium, 1998.
70. Stucchi, M.; Rovida, A.; Gomez Capera, A.A.; Alexandre, P.; Camelbeeck, T.; Demircioglu, M.B.; Gasperini, P.; Kouskouna, V.; Musson, R.M.W.; Radulian, M.; et al. The SHARE European Earthquake Catalogue (SHEEC) 1000–1899. *J. Seismol.* **2013**, *17*, 523–544. [CrossRef]
71. SHEEC Earthquake Catalogue 1900–2006. Available online: http://sheec-1900-2006.gfz-potsdam.de/ (accessed on 1 October 2017).
72. USGS Earthquake Catalogue. Available online: https://earthquake.usgs.gov/earthquakes/search/ (accessed on 10 December 2019).
73. Shebalin, N.V.; Karnik, V.; Hadzievski, D. *UNDP/UNESCO Survey of the Seismicity of the Balkan Region—Catalogue of Earthquakes*; Printing Office of the University Kiril and Metodij: Skopje, North Macedonia, 1974.

74. Ciocârdel, R.; Esca, A. Essai de synthese des donnees, actuelles concertant les mouvements verticaux recents de l'ecorce terrestre en Roumanie. *Rev. Roum. Geol. Geophys. Geogr. Ser. Geophys.* **1966**, *10*, 5–32.
75. Brandabur, T.; Ghenea, C.; Săndulescu, M.; Ştefănescu, M. Harta neotectonică a României, 1:1,000,000. In *Atlasul Geologic*; Foaia Nr. 7; Geological Institute of Romania: Bucharest, Romania, 1971.
76. Visarion, M.; Săndulescu, M.; Drăgoescu, I.; Drăghici, M.; Cornea, I.; Popescu, M. *Harta Mişcărilor Crustale Verticale Recente, 1:1,000,000*; Geological Institute of Romania: Bucharest, Romania, 1977.
77. Cornea, I.; Drăgoescu, I.; Popescu, M.; Visarion, M. Harta mişcărilor crustale verticale recente pe teritoriul R.S. România. *St. Cerc. Geol. Geophys. Geogr. Geophys.* **1979**, *17*, 3–20.
78. Popescu, M.N.; Drăgoescu, I. New map of recent vertical crustal movements in Romania, 1:1,000,000. *Rev. Roum. Geol. Geophys. Et Geogr. Ser. Geophys.* **1986**, *30*, 3–10.
79. Blewitt, G.; Lavallee, D.; Clarke, P.J.; Nurutdinov, K. A New Global Mode of Earth Deformation: Seasonal Cycle Detected. *Science* **2002**, *294*, 2342–2345. [CrossRef]
80. van Dam, T.; Blewitt, G.; Heflin, M. Atmospheric pressure loading effects on Global Positioning System coordinate determinations. *J. Geophys. Res.* **1994**, *99*, 23939–23950. [CrossRef]
81. Scherneck, H.G. A parametrized Solid Earth Tide Model and Ocean Tide Loading Effects for global geodetic baseline measurements. *Geophys. J. Int.* **1991**, *106*, 677–6941991. [CrossRef]
82. Mangiarotti, S.; Cazenave, A.; Soudarin, L.; Cretaux, J.F. Annual vertical crustal motions predicted from surface mass redistribution and observed by space geodesy. *J. Geophys. Res.* **2001**, *106*, 4277–4291. [CrossRef]
83. Miller, M.M.; Melbourne, T.; Johnson, D.J.; Sumner, W.Q. Periodic Slow Earthquakes from the Cascadia Subduction Zone. *Science* **2002**, *295*, 2423. [CrossRef] [PubMed]
84. Alba, S.; Weldon, R.J.; Livelybrooks, D.; Schmidt, D.A. Cascadia ETS Events Seen in Tidal Records (1980–2011). *Bul. Seis. Soc. Am.* **2019**, *109*, 812–821. [CrossRef]
85. Barlik, M.; Borza, T.; Busics, I.; Fejes, I.; Pachelski, W.; Rogowski, J.; Sledzinski, J.; Zielinski, J. Central Europe Regional Geodynamics Project. *Rep. Geod.* **1994**, *2*, 7–24.
86. Fejes, I. Consortium for Central European GPS Geodynamic Reference Network (CEGRN Consortium). In *The Adria Microplate: GPS Geodesy, Tectonics, and Hazards*; Pinter, N., Grenerczy, G., Weber, J., Stein, S., Medak, D., Eds.; Springer: Dordrecht, The Netherlands, 2006; pp. 183–194.
87. Caporali, A.; Aichhorn, C.; Becker, M.; Fejes, I.; Gerhatova, L.; Ghitau, D.; Grenerczy, G.; Hefty, J.; Krauss, S.; Medak, K.; et al. Geokinematics of Central Europe: New insights from the CERGOP-2/Environment Project. *J. Geodyn.* **2008**, *45*, 246–256. [CrossRef]
88. Hefty, J. Work-Package 5 of the CERGOP-2/Environment: GPS data analysis and the definition of reference frames activity report April 2004–September 2004. *Rep. Geod.* **2004**, *4*, 23–34.
89. Hefty, J. Work-Package 7 of the CERGOP-2/Environment: Geokinematical modelling and strain analysis activity report April 2004–September 2004. *Rep. Geod.* **2004**, *4*, 39–42.
90. Săndulescu, M.; Krautner, H.; Borcoş, M.; Năstăseanu, S.; Patrulius, D.; Ştefănescu, M.; Ghenea, C.; Lupu, M.; Savu, H.; Bercia, I.; et al. Harta geologică a României, 1:1,000,000. In *Atlasul Geologic*; Foaia Nr. 1; Romanian Institute of Geology and Geophysics: Bucharest, Romania, 1978.
91. Oncescu, N. *Geologia României*; Editura Tehnică: Bucharest, Romania, 1965; p. 534.
92. EMODNET Bathymetry Data Portal. Available online: https://portal.emodnet-bathymetry.eu/ (accessed on 10 May 2020).
93. Stanciu, I.M.; Ioane, D.; Seghedi, A. Chapter 1. Geographical setting, Geomorphological and Geotectonic framework of Bucharest City. In *Bucharest—European Capital City with the Most Vulnerable Response to a Strong Earthquake*; Ionescu, C., Radulian, M., Bălă, A., Eds.; Editura Cetatea de Scaun: Târgoviște, Romania, 2022; pp. 13–31, ISBN 978-606-537-601-4/ebook 978-606-537-602-1. [CrossRef]
94. Keller, E.A.; Pinter, N. *Active Tectonics: Earthquakes, Uplift, and Landscape*, 2nd ed.; Prentice Hall: Upper Saddle River, NJ, USA, 2002; p. 362.
95. Fielitz, W.; Seghedi, I. Late Miocene–Quaternary volcanism, tectonics and drainage system evolution in the East Carpathians, Romania. *Tectonophysics* **2005**, *410*, 111–136. [CrossRef]
96. Panaiotu, C.G.; Panaiotu, E.C.; Grama, A.; Necula, C. Paleoclimatic record from a loess-paleosol profile in southeastern Romania. *Phys. Chem. Earth Part A Solid Earth Geod.* **2001**, *26*, 893–898. [CrossRef]
97. Timar-Gabor, A.; Vasiliniuc, Ş.; Vandenberghe, D.; Cosma, C. Absolute Dating of Romanian Loess Using Luminescence Techniques: Palaeoclimatic Implications. 2009. Available online: https://www.researchgate.net/publication/292436437 (accessed on 15 September 2019).
98. van der Hoeven, A.; Schmitt, G.; Dinter, G.; Mocanu, V.; Spakman, W. GPS probes the kinematics of the Vrancea seismogenic zone. *EOS* **2004**, *85*, 185–196. [CrossRef]
99. van der Hoeven, A.; Mocanu, V.; Spakman, W.; Nutto, M.; Nuckelt, A.; Mațenco, L.; Munteanu, L.; Marcu, C.; Ambrosius, B. Observation of present-day tectonic motions in the Southeastern Carpathians: Results of the ISES/CRC-461 GPS measurements. *Earth Planet. Sci. Lett.* **2005**, *239*, 177–184. [CrossRef]

100. Munteanu, L. Cinematica blocurilor tectonice din arealul vrâncean, utilizând tehnologie modernă satelitară de mare precizie. In *Cercetări Privind Managementul Dezastrelor Generate de Cutremurele Românești*; Mărmureanu, G., Ed.; Tehnopress: Iaşi, Romania, 2009; ISBN 973-702-7014-9.
101. Milev, G.; Vassileva, K. Geodynamics of the Balkan Peninsula and Bulgaria. In Proceedings of the International Symposium on Strong Vrancea Earthquakes and Risk Mitigation, Bucharest, Romania, 4–6 October 2007; pp. 55–70.
102. Kotzev, V.; Nakov, R.; Burchfiel, B.C.; King, R. NW Bulgaria—The Northern Boundary of the Aegean Extensional Domain. In *Vistas for Geodesy in the New Millennium. International Association of Geodesy Symposia*; Ádám, J., Schwarz, K.P., Eds.; Springer: Berlin, Germany, 2002; Volume 125, pp. 501–505. [CrossRef]
103. Kotzev, V.; Nakov, R.; Burchfiel, B.C.; King, R.W.; Reilinger, R. GPS study of active tectonics in Bulgaria: Results from 1996 to 1998. *J. Gcodynamics* **2001**, *31*, 189–200. [CrossRef]
104. Papanikolaou, D.; Barghathi, H.; Dabovski, C.; Dimitriu, R.G.; El-Hawat, A.; Ioane, D.; Kranis, H.; Obeidi, A.; Oaie, G.; Seghedi, A.; et al. TRANSMED Transect VII: East European Craton—Scythian Platform—Dobrogea—Balkanides—Rhodope Massif—Hellenides—East Mediterranean—Cyrenaica. In *The TRANSMED Atlas—The Mediterranean Region from Crust to Mantle*; Cavazza, W., Roure, F., Spakman, W., Stampfli, G.M., Ziegler, P.A., Eds.; Springer: Berlin/Heidelberg, Germany, 2004.
105. Nyst, M.; Thatcher, W. New constraints on the active tectonic deformation of the Aegean. *J. Geophys. Res. B Solid Earth* **2004**, *109*, 1–23. [CrossRef]
106. Cloetingh, S.A.P.L.; Ziegler, P.A.; Bogaard, P.J.F.; Andriessen, P.A.M.; Artemieva, I.M.; Bada, G.; van Balen, R.T.; Beekman, Z.; Ben-Avraham, F.; Brun, J.-P.; et al. TOPO-EUROPE: The geoscience of coupled deep Earth-surface processes. *Glob. Planet. Chang.* **2007**, *58*, 1–118. [CrossRef]
107. McClusky, S.; Balassanian, S.; Barka, A.; Demir, C.; Ergintav, S.; Georgiev, I.; Gurkan, O.; Hamburger, M.; Hurst, K.; Kahle, H.; et al. Global Positioning System constraints on plate kinematics and dynamics in the eastern Mediterranean and Caucasus. *J. Geophys. Res.* **2000**, *105*, 5695. [CrossRef]
108. Müller, M.D.; Geiger, A.; Kahle, H.G.; Veis, G.; Billiris, H.; Paradissis, D.; Felekis, S. Velocity and deformation fields in the North Aegean domain, Greece, and implications for fault kinematics, derived from GPS data 1993–2009. *Tectonophysics* **2013**, *597–598*, 34–49. [CrossRef]
109. Vassileva, K.; Atanasova, M. Study of plate transition boundaries in Bulgaria from GPS. In Proceedings of the SES 2014 Tenth Anniversary Scientific Conference with International Participation Space, Ecology, Safety, Sofia, Bulgaria, 12–14 November 2014; pp. 356–362.
110. Lazos, I.; Pikridas, C.; Chatzipetros, A.; Pavlides, S. Determination of local active tectonics regime in central and northern Greece, using primary geodetic data. *Appl. Geomat.* **2020**, *13*, 3–17. [CrossRef]
111. Lowman, P.D. Global Tectonic and Volcanic Activity for the Last One Million Years. 1997. Available online: https://core2.gsfc.nasa.gov/research/lowman/lowman.html (accessed on 7 September 2016).
112. Tectonic Plates Geodynamic Model of California Institute of Technology—Tectonics Observatory. Available online: www.tectonics.caltech.edu (accessed on 10 May 2019).
113. Bird, P. An updated digital model of plate boundaries. *Geoch. Geophys. Geosys.* **2003**, *4*, 1027. [CrossRef]
114. Hristov, V.; Totomanov, I.; Vrablianski, B.; Burilkov, T. *Map of the Recent Vertical Movements in Bulgaria*; Central Geodetic Laboratory BAS, Geological Institute BAS: Sofia, Bulgaria, 1973.